The EMBO Journal (2006) 25, 2919–2929 | © 2006 European Molecular Biology Organization | All Rights Reserved 0261-4189/06
www.embojournal.org

THE EMBO JOURNAL

Two conformations of a crystalline human tRNA synthetase–tRNA complex: implications for protein synthesis

Xiang-Lei Yang[1,*], Francella J Otero[1], Karla L Ewalt[1], Jianming Liu[1], Manal A Swairjo[1], Caroline Köhrer[2], Uttam L RajBhandary[2], Robert J Skene[3], Duncan E McRee[3,4] and Paul Schimmel[1]

[1]Department of Molecular Biology, The Scripps Research Institute, La Jolla, CA, USA, [2]Massachusetts Institute of Technology, Department of Biology, Cambridge, MA, USA and [3]Syrrx, Inc., San Diego, CA, USA

Aminoacylation of tRNA is the first step of protein synthesis. Here, we report the co-crystal structure of human tryptophanyl-tRNA synthetase and $tRNA^{Trp}$. This enzyme is reported to interact directly with elongation factor 1α, which carries charged tRNA to the ribosome. Crystals were generated from a 50/50% mixture of charged and uncharged $tRNA^{Trp}$. These crystals captured two conformations of the complex, which are nearly identical with respect to the protein and a bound tryptophan. They are distinguished by the way tRNA is bound. In one, uncharged tRNA is bound across the dimer, with anticodon and acceptor stem interacting with separate subunits. In this cross-dimer tRNA complex, the class I enzyme has a class II-like tRNA binding mode. This structure accounts for biochemical investigations of human TrpRS, including species-specific charging. In the other conformation, presumptive aminoacylated tRNA is bound only by the anticodon, the acceptor stem being free and having space to interact precisely with EF-1α, suggesting that the product of aminoacylation can be directly handed off to EF-1α for the next step of protein synthesis.

The EMBO Journal (2006) **25,** 2919–2929. doi:10.1038/sj.emboj.7601154; Published online 25 May 2006
Subject Categories: proteins; structural biology
Keywords: aminoacyl-tRNA synthetase; crystal structure; dual conformations; human TrpRS; tRNA

Introduction

Through aminoacylations of tRNAs, the genetic code relationship of amino acids to specific nucleotide triplets was fixed, and then maintained throughout the development of the tree of life with its three great kingdoms—archaea, bacteria, and eukarya. Aminoacylations are catalyzed by tRNA synthetases, enzymes that were divided into two classes—class I and class II—at an early stage in evolution. The architectural features of the active site and mode of tRNA binding distinguish the two classes, and are thought to have played a role in the mechanism of establishment of the early code (Carter, 1993; Cusack, 1995; Arnez and Moras, 1997; Ribas de Pouplana and Schimmel, 2001; Schimmel and Ribas de Pouplana, 2001). Further pressures of evolution resulted in the enzymes acquiring other biological functions, particularly in eukaryotes (Myers *et al*, 2002; Torres-Larios *et al*, 2002; Sampath *et al*, 2004; Yang *et al*, 2004; Park *et al*, 2005), and developing mechanisms to efficiently process charged tRNAs for protein synthesis. Here, we report a crystal structure that suggests how some of these mechanisms may operate.

Structures of all 20 tRNA synthetases are known, with some showing details of interactions with tRNA and how the enzymes accomplish editing reactions (Sankaranarayanan and Moras, 2001). Not understood from a structural perspective are many temporal phenomena, such as the process of distinguishing and releasing charged versus uncharged tRNA and how the synthetase-directed system of aminoacylation is integrated into the rest of protein synthesis. After formation of charged tRNA (AA-tRNA), elongation factor Tu in bacteria, or its ortholog EF-1α in eukaryotes, binds AA-tRNA and delivers it to the ribosome. Apart from its long-standing intuitive appeal, the idea that charged tRNA may be directly handed off to an elongation factor gained some interest with the discovery that human TrpRS (Sang Lee *et al*, 2002), among other mammalian tRNA synthetases (Negrutskii *et al*, 1996, 1999; Petrushenko *et al*, 2002), had a specific association with EF-1α.

We set out to investigate human TrpRS, with interest in the temporal events of aminoacylation and the possibility that these events could be related to the next step of protein synthesis. There are different ways in which this problem can be addressed, but in this particular instance, we followed a strategy that took advantage of the serendipitous observation where both charged and uncharged tRNA were present with the homodimeric class I enzyme in the solution. This situation allowed for both forms of tRNA to bind to and potentially crystallize with the synthetase and, in this scenario, to give a picture of how the enzyme might transition from one form to the other. At the same time, we hoped to uncover a structure that would also give insight into whether and how an interaction with EF-1α could occur with the synthetase–tRNA complex.

Results

Sample containing both charged and uncharged tRNAs

To encourage formation of distinct conformations of the synthetase–tRNA complex, we undertook a strategy to examine conditions favoring uncharged tRNA (adding tRNA

*Corresponding author. Department of Molecular Biology, The Scripps Research Institute, BCC-379, 10550 North Torrey Pines Road, La Jolla, CA 92037, USA. Tel.: +1 858 784 8976; Fax: +1 858 784 8990; E-mail: xlyang@scripps.edu
[4]Present address: ActiveSight, 4045 Sorrento Valley Boulevard, San Diego, CA 92121, USA

Received: 12 January 2006; accepted: 27 April 2006; published online: 25 May 2006

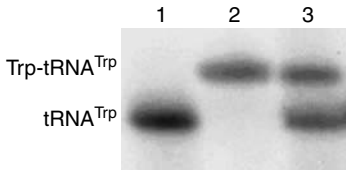

Figure 1 Analysis of tRNA^{Trp} using acid urea PAGE/Northern blot. Lane 1: uncharged tRNA^{Trp}. Lane 2: sample containing approximately equimolar of TrpRS and tRNA^{Trp}, 5 mM tryptophan and 10 mM ATP. Lane 3: sample containing approximately equimolar of TrpRS and tRNA^{Trp}, 5 mM tryptophan and 10 mM AMPPNP.

alone), fully charged tRNA (ATP + Trp + tRNA) or mixtures of uncharged and charged tRNA (AMPPNP + Trp + tRNA) in complex with human TrpRS. Mixing approximately equimolar tRNA with the synthetase yielded uncharged tRNA, while adding excess tryptophan and ATP, gave fully aminoacylated tRNA^{Trp} (Figure 1). When we added excess tryptophan and AMPPNP to the equimolar TrpRS and tRNA^{Trp} mixture, approximately 50% of tRNA^{Trp} was aminoacylated (Figure 1). (AMPPNP is an analog of ATP that has a phosphoramidate linkage between the β- and γ-phosphate positions. As the critical (for adenylate formation) linkage between the α- and β-phosphate was unaltered, AMP-PNP was a substrate for aminoacylation and yet has weaker activity than ATP (data not shown)) Presumably, the reduced forward rate of aminoacylation with AMPPNP combined with spontaneous deacylation of the charged tRNA resulted in an equilibrium tRNA pool that was half charged and half uncharged.

Two distinct tRNA conformations

Complex samples with uncharged, 50% charged, and fully charged tRNAs were used for crystallization. Samples with homogenously uncharged and charged tRNAs did not yield diffracting crystals. Interestingly, the sample with a 50/50% mixture of charged and uncharged tRNA^{Trp} in complex with approximately equimolar of human TrpRS and excess tryptophan and AMPPNP yielded orthorhombic crystals, which diffracted to 2.9 Å with space group $I2_12_12_1$. The structure was solved by the single wavelength anomalous dispersion (SAD) method using a selenium-labeled crystal. The asymmetric unit contains two enzyme subunits, with each subunit having bound tRNA^{Trp} and tryptophan. Each tRNA in the asymmetric unit interacts with one monomer but not the other (Figure 2A). The two enzyme monomers of the asymmetric unit, although related by a pseudo-two-fold symmetry, are not the biological dimer. The biological dimer of each monomer–tRNA pair can be generated by a crystallographic two-fold symmetry operation, resulting in two distinct dimeric tRNA complexes of TrpRS (Figure 2B and C). Although the conformations of the enzyme monomers are virtually identical (r.m.s. deviation of 0.42 Å for 387 Cα atoms of TrpRS monomer), the two complexes are sharply different.

This difference is seen in the conformations of their tRNAs (Figure 3A and B). In one complex, two tRNA molecules bind symmetrically across the surface of the biological dimer. For this complex, each tRNA has its anticodon loop and acceptor stem interacting with different subunits (Figure 2B) (as also seen in the structure of the close homolog TyrRS in complex with tRNA^{Tyr} (Yaremchuk *et al*, 2002; Kobayashi *et al*, 2003)).

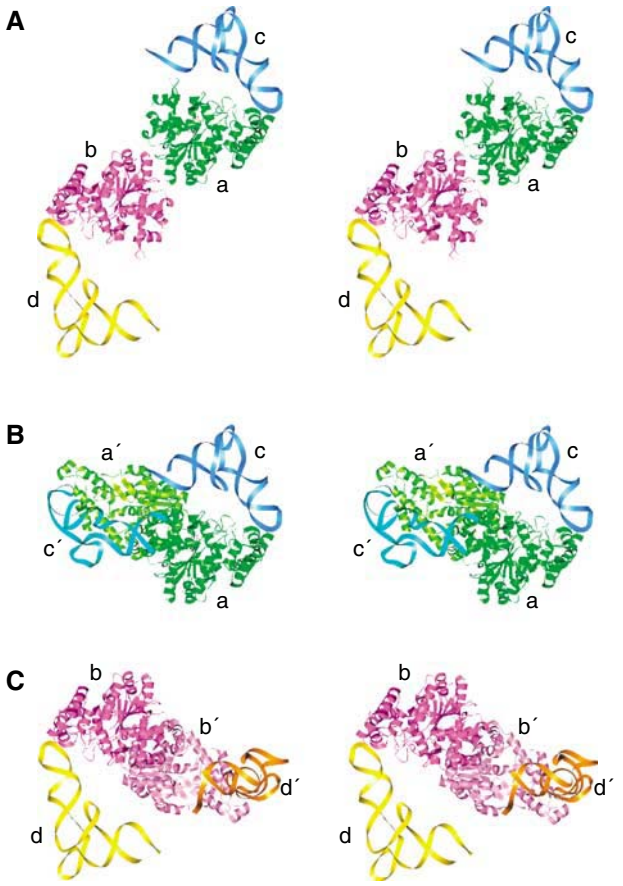

Figure 2 (**A**) The asymmetric unit of the human TrpRS–tRNA^{Trp} crystal. It contains two enzyme monomers, a and b, and two tRNAs, c and d, that interact with a and b, respectively. (**B**) The association complex generated by applying a crystallographic two-fold symmetry operation to molecules a and c. (**C**) The dissociation complex generated by applying a crystallographic two-fold symmetry operation to molecules b and d.

However, in the other complex, the acceptor stem of each tRNA was dissociated from the synthetase while the anticodon loop was still attached (Figure 2C). The two conformations were named 'association complex' and 'dissociation complex', respectively.

When the synthetases are superimposed, as seen in Figure 3, the conformations of the associative tRNA and the dissociative tRNA overlap only at the anticodon loop. The rest of the L-shaped tRNA planes gradually separate from each other forming an approximate 25° angle in between the anticodon-D arms, while the acceptor-TψC arms are completely separated and parallel. In fact, the acceptor-TψC arms and the D-loops can be superimposed, but not simultaneously with the anticodon stem-loops. The r.m.s. deviation for the acceptor-TψC arm and the D-loop is 1.56 Å for 46 phosphorus atoms (C3–C23, G45–G70), and 1.00 Å for the anticodon stem-loop (G26–A44). However, superimposing both regions gave an r.m.s. deviation of 2.89 Å for a total of 65 phosphorus atoms. The difference can best be described as a slight curvature occurring over the joint that connects the anticodon stem and the D stem (of anticodon-D arm) in the dissociative compared to the associative tRNA. Thus, unlike the two enzyme monomers, the overall tRNA conformations are not as similar.

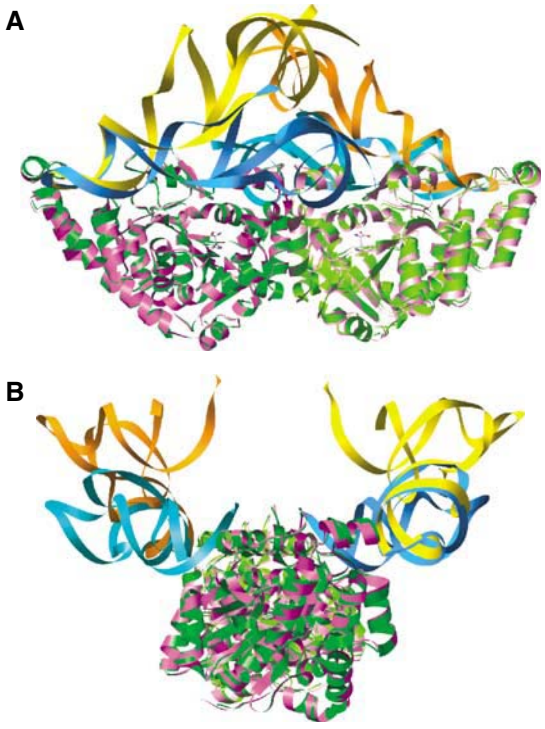

Figure 3 (**A**) Superposition of the association complex and the dissociation complex by overlapping their proteins. (**B**) Another view of the superposition with a 90° rotation along the *y*-axis.

For the 'association' tRNA, except for the 3′-end CCA(74–76) trinucleotide, the entire acceptor stem including the unpaired base (A73) is resolved. Although the amino-acid attachment site is completely disordered, A73 is close to the active site pocket that holds bound tryptophan. In contrast, the 'dissociation' tRNA is more disordered at the acceptor stem. In addition to the 3′-CCA, A73 and the first two base pairs of the acceptor stem (G1–C72 and A2–U71) are partially disordered with dissociation of the base pairs. Presumably, the greater disorder of the dissociation complex arises because of the lack of interactions between the acceptor stem and the synthetase.

Structure of protein in association and dissociation complexes

Alignment of the sequence of the 471 amino-acid human TrpRS with its 328 amino-acid *Bacillus stearothermophilus* ortholog is shown in Figure 4, with secondary structure elements for the human enzyme shown over the sequence. Specific landmarks, such as the N-terminal appended domain, eukaryote-specific patch, Rossmann fold catalytic domain, and anticodon recognition domain, are also shown. As previously noted, the N-terminal appended domain and the eukaryote-specific patch are missing from the bacterial ortholog and largely account for its smaller size.

The first 81 residues, which include the N-terminal appended domain, are completely disordered in these structures of human TrpRS. The N-terminal appended domain is a member of the WHEP-TRS conserved domain family (Bateman *et al*, 2002). Homologues of this domain are found in several other human aminoacyl-tRNA synthetases, including those for glycine, histidine, aspartate, lysine, and methionine, and as a linker domain fusing together the two synthetases of the bifunctional glutamyl-prolyl-tRNA synthetase (Glu-ProRS) (Lee *et al*, 2004; Sampath *et al*, 2004; Yang *et al*, 2004). The WHEP-TRS domain adopted a helix–turn–helix structure in a crystal structure of human TrpRS (in complex with Trp-AMP) (Yang *et al*, 2003) and in the NMR structure of the isolated WHEP-TRS domain of human Glu-ProRS (Jeong *et al*, 2000). Although the WHEP-TRS domain of human Glu-ProRS was reported to weakly bind tRNA (Jeong *et al*, 2000), the homologous N-terminal domain in human TrpRS is completely disordered in both complexes seen here, suggesting the absence of a strong interaction between this domain and $tRNA^{Trp}$. (The integrity of TrpRS was confirmed by gel electrophoresis of the dissolved crystals (data not shown).) Our biochemical analyses support the lack of significant contribution to $tRNA^{Trp}$ binding by the N-terminal domain. Deletion of this domain, as in mini-TrpRS (Wakasugi *et al*, 2002), did not change the apparent K_m for tRNA and only slightly changed the k_{cat} for aminoacylation compared to the full-length enzyme (K_m 1.3 μM, k_{cat} 1.1 s^{-1}, full-length TrpRS; K_m 1.4 μM, k_{cat} 3.1 s^{-1}, mini-TrpRS). The conformation of the WHEP-TRS domain adopted in previous human TrpRS structure (Yang *et al*, 2003) does not seem to interfere with $tRNA^{Trp}$ binding in both complexes. The fact that this domain is disordered here, and was resolved in only one of the two TrpRS subunits (Yang *et al*, 2003) indicates that the WHEP-TRS domain is flexible relative to the rest of the enzyme and may be involved in functions other than aminoacylation.

The eukaryote-specific patch (E82–K154) is intimately associated with and extends the Rossmann fold (P155–S353) (Figure 5A). The β1–β2 hairpin structure at the N-terminus of the patch is adjacent to the tryptophan binding pocket and the KMSAS loop. Deletion of this hairpin, as in T2-TrpRS, results in severe reduction of aminoacylation activity (data not shown). The anticodon recognition domain (D354–F468, with the C-terminus after F468 being disordered) consists of six α-helices, and is linked to the Rossmann fold via the KMSAS loop. As seen in previous structures of TrpRS (Doublie *et al*, 1995; Ilyin *et al*, 2000; Retailleau *et al*, 2001; Retailleau *et al*, 2003; Yang *et al*, 2003; Kise *et al*, 2004; Yu *et al*, 2004), an insertion (known as CP1) into the Rossmann fold is used to form the dimer interface. The conformation of TrpRS in both complexes closely resembles that of the previously reported Trp–AMP complex (Yang *et al*, 2003), including the KMSAS loop region, with r.m.s. deviation of 0.49 Å for 386 Cα atoms. In both complexes, no electron density of AMPPNP is found, yet the KMSAS loop is stabilized by interactions with the β1–β2 hairpin and a sulfate ion (from the precipitant ammonium sulfate) that could mimic one of the phosphate groups of ATP or AMPPNP.

Acceptor stem recognition in the association complex

In the association complex, the acceptor stem of $tRNA^{Trp}$ interacts with the extended Rossmann fold domain of TrpRS at the major groove side. Interaction with the major groove side of the acceptor stem is a characteristic mode of interaction for class II aaRSs and, shared only with TyrRS (Lee and RajBhandary, 1991; Bedouelle *et al*, 1993; Yaremchuk *et al*, 2002; Kobayashi *et al*, 2003), among other class I tRNA synthetases (Arnez and Moras, 1997). The anticodon loop of $tRNA^{Trp}$ interacts with the anticodon recognition domain of

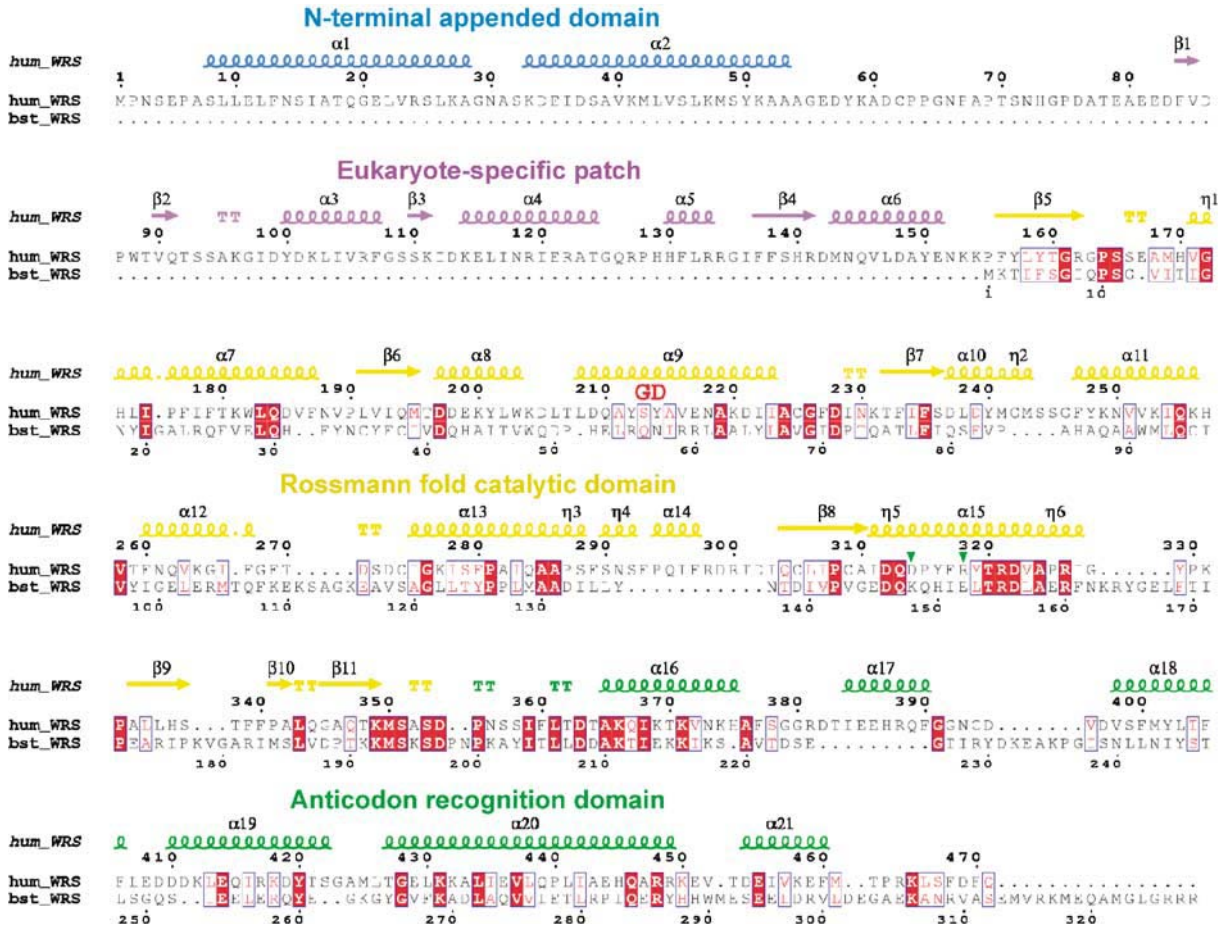

Figure 4 Sequence alignment of TrpRSs from human and *B. stearothermophilus*, with the secondary structure elements derived from the human TrpRS structure shown over the sequence. The secondary structure elements from different domains were colored with a scheme that is kept throughout the rest the figures. The secondary structure of the N-terminal appended domain is adapted from a previous crystal structure of human TrpRS (Yang *et al*, 2003), as this domain is disordered here in both association and dissociation complexes. A sequence variant TrpRS(G213D214) (Ewalt *et al*, 2005) was used for the crystal structure analysis.

the other subunit of the TrpRS dimer (Figure 5A). Although $tRNA^{Trp}$ from different taxa bear the same anticodon, human TrpRS does not significantly charge $tRNA^{Trp}$ from bacteria or vice versa (Guo *et al*, 2002). The major identity element on $tRNA^{Trp}$ that determines the species-specificity is N73 in the acceptor stem (Xue *et al*, 1993, 2001). Archaeal and most eukaryotic $tRNA^{Trp}$, including human, have A73, whereas $tRNA^{Trp}$ from bacteria has G73 (Guo *et al*, 2002).

Residues from both the eukaryote-specific patch and from the Rossmann fold approach the major groove of the acceptor stem. Most of the interactions between TrpRS and the acceptor stem involve the phosphate backbone (Figure 6A). Several positively charged arginine and lysine residues from the extended Rossmann fold domain are gathered in space so as to be near these negatively charged phosphate groups. For example, R141, R318, R321, and K331 are close to the phosphate group of G1, R326 is close to the phosphate groups of G68 and G69, and K264 is close to the phosphate of U71. Among those, R326 and K331 are within hydrogen-bonding distance for interacting with their respective phosphate groups. In addition, the phosphate oxygens of G70 form hydrogen bonds with the side chains of T259 and N261 of the CP1 insertion. Except for R321 and R326, none of those amino-acid residues are conserved in bacterial TrpRS (Figure 4).

With the 3′-end CCA tri-nucleotide disordered, the adjacent A73 nucleotide was slightly disordered. Nevertheless, R318 can specifically discriminate the major identity element A73 from G73, the sequence found in bacterial $tRNA^{Trp}$ (Figure 6A). In fact, R318, located on helix α15 of the Rossmann fold, is the only residue that has a base-specific interaction in the association complex. The conformation of the R318 side chain is stabilized by a hydrogen-bonding network that involves D314 on α15 as well as F107 and R141 from the eukaryote-specific patch on α3 and β4, respectively (Figure 6A). (All four residues in the hydrogen-bonding network are highly conserved throughout eukaryotes and archaea.) Meanwhile, the guanidino group of R318 stacks on top of G1, and donates a hydrogen bond to the N1 atom of A73 (Figure 6A and B). Such a hydrogen bond cannot be formed with G73, because the N1 of guanine has a covalently attached hydrogen atom that can only act as a hydrogen bond donor.

Previous work showed that human TrpRS has a preference of A>C>U>G at position 73 (Guo *et al*, 2002). The interaction scheme between R318 and A73 can explain this observation. Both A and C have a nonprotonated N, while

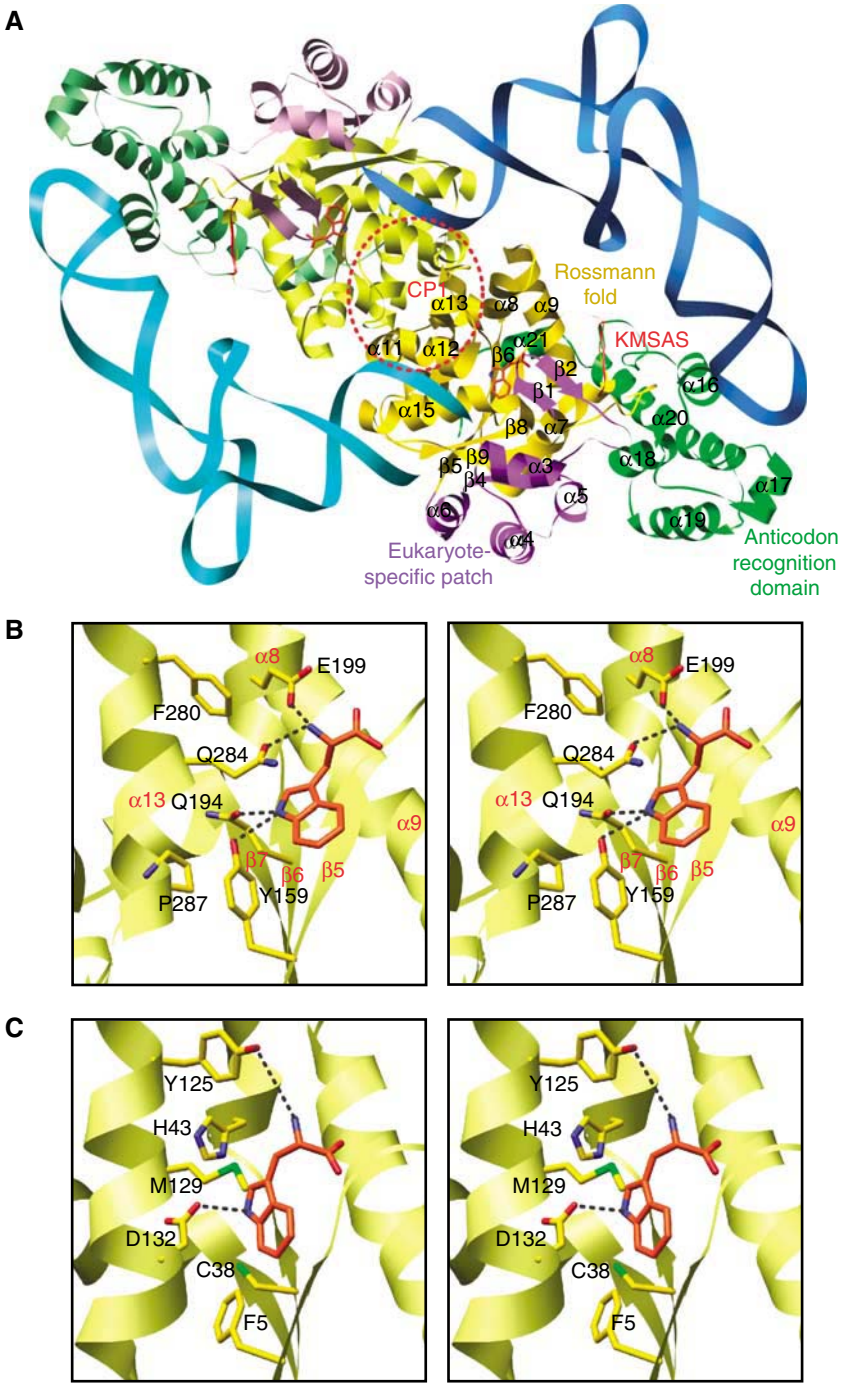

Figure 5 (**A**) Structure of the association complex with two tRNA molecules (light and dark blue) binding across the TrpRS dimer. A tryptophan is bound in each TrpRS subunit. (**B**) Stereoview of the tryptophan binding site of human TrpRS. (**C**) Stereoview of the tryptophan binding site of *B. stearothermophilus* TrpRS.

U and G have NH at the N1 position of purine or the equivalent N3 position of pyrimidine. Being larger than pyrimidine, a purine (A or G) places its N1 group closer to R318 than does the N3 of pyrimidine (C or U), and therefore has more favorable (for A) or unfavorable (for G) interactions than do the pyrimidine bases.

Interestingly, while R318 of human TrpRS is highly conserved among eukaryotes and archaea, the corresponding residue in bacterial TrpRSs is strictly E (Jia *et al*, 2004) (Figure 4). Importantly, the functional group of glutamate is usually deprotonated, under physiological conditions, and can only accept a hydrogen bond, and thus recognize the protonated N1 position of G73 (Figure 6C). Therefore, the same position on TrpRS could in principle be used for specifically recognizing G73 in bacteria, and for recognizing A73 in eukaryotes and archaea. Remarkably, a point mutation at this position (E153K) in *Bacillus subtilis* TrpRS (similar to arginine, the lysine side chain can only donate a hydrogen bond) switched the species-specificity, and was reported to prefer human $tRNA^{Trp}$ to its cognate

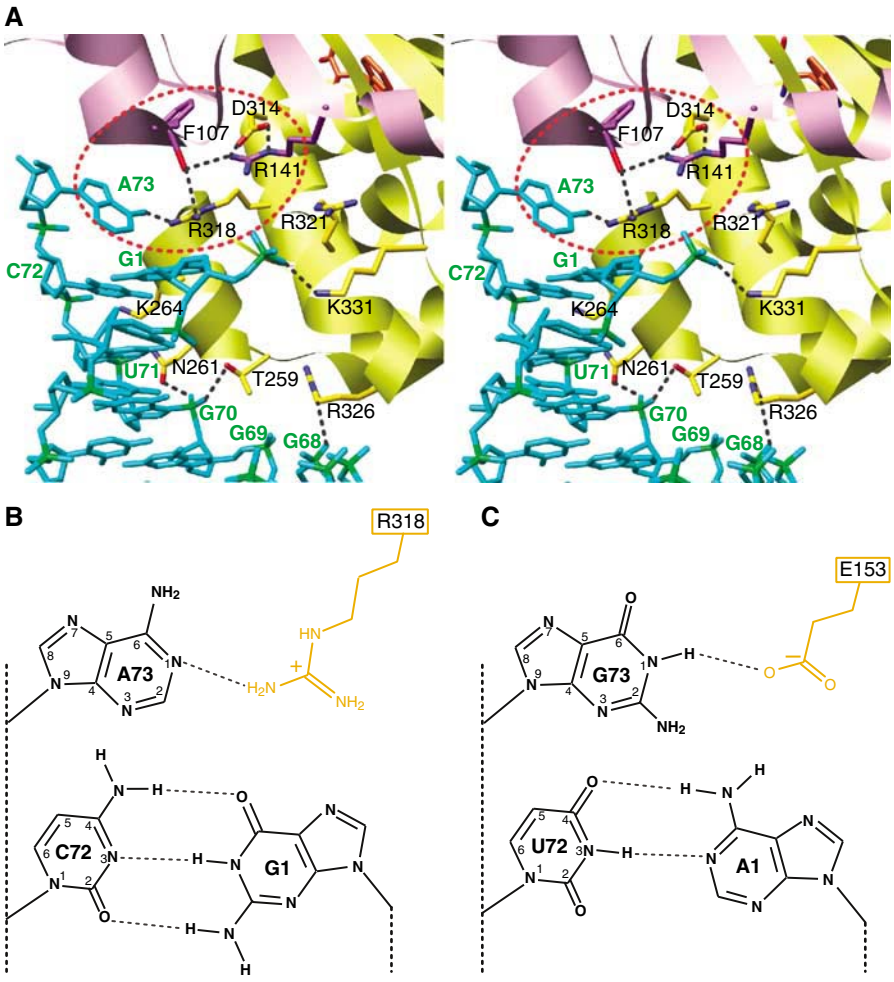

Figure 6 (**A**) Stereoview of TrpRS–tRNA^{Trp} interactions at the acceptor stem. (tRNA^{Trp} is colored in blue with phosphorus atoms in green. The eukaryote-specific patch is in purple, and the Rossmann fold is in yellow.) R318 makes a base-specific interaction with the major identity element A73. The conformation of R318 is stabilized by a hydrogen-bonding network involving residues F107, R141 and D314. (**B**) Schematic drawing of A73 recognition by R318 of human TrpRS. (**C**) E153 of *B. subtilis* TrpRS, the corresponding residue of R318 of human TrpRS, can recognize G73, the sequence in prokaryotic tRNA^{Trp}.

bacterial tRNA^{Trp} (Jia *et al*, 2004). A double mutation in *B. subtilis* TrpRS (K149D/E153R) was even more effective in switching species-specificity than the point mutation E153K. K149 of *B. subtilis* TrpRS corresponds to D314 of human TrpRS, which is involved in the hydrogen-bonding network with R318. One might expect that D149 of K149D/E153R *B. subtilis* TrpRS would help to position R153 for A73 recognition, so as to achieve specificity swapping. However, because F107 and R141 (which bridge D314 and R318 in human TrpRS) are absent in bacterial TrpRS (Figure 4), the interaction between D149 and R153 in K149D/E153R *B. subtilis* TrpRS must be different.

It was pointed out previously that the preference for A73 in tRNA^{Trp} by eukaryotic and archaeal TrpRS is much weaker than the preference for G73 by bacterial TrpRS (Guo *et al*, 2002). Our structural observation that R318 is the only residue that recognizes A73 is consistent with the biochemical data. It is likely that bacterial TrpRS has more base-specific interactions with the acceptor stem, which collectively enhance the preference for G73.

All of the aforementioned interactions with the acceptor stem are missing in the dissociation complex.

Anticodon recognition in both complexes

Interactions with the anticodon in the association and dissociation complexes are almost identical. The anticodon of tRNA^{Trp} is embraced by helices α16, α17, and α20 of the anticodon recognition domain in both the association and dissociation complexes of TrpRS, with all three bases being specifically recognized (Figure 7A). The conformation of the anticodon resembles that of complexed tRNA^{Tyr} from *M. jannaschii* (Kobayashi *et al*, 2003). The first base—C34—is flipped out, while the second—C35—and the third—A36—remain stacked. The O2, N3, and N4 atoms of C34 are recognized by main-chain nitrogens of T427 and G428 from α20, and by the main-chain oxygen of R381 from the loop between α16 and α17, respectively (Figure 7B). For C35, O_2 is recognized by the ε-amino of K431 from α20, N3 is recognized by the OH of S378, and N4 interacts with main-chain oxygens of both G380 and R381 (Figure 7C). While the first two bases of the anticodon are saturated by hydrogen-bonding interactions with the protein, recognition of the third base A36 is less stringent. The main-chain nitrogen of S378 and the carboxyl group of D382, respectively, take up two of the four possible hydrogen-bonding positions N3 and N6

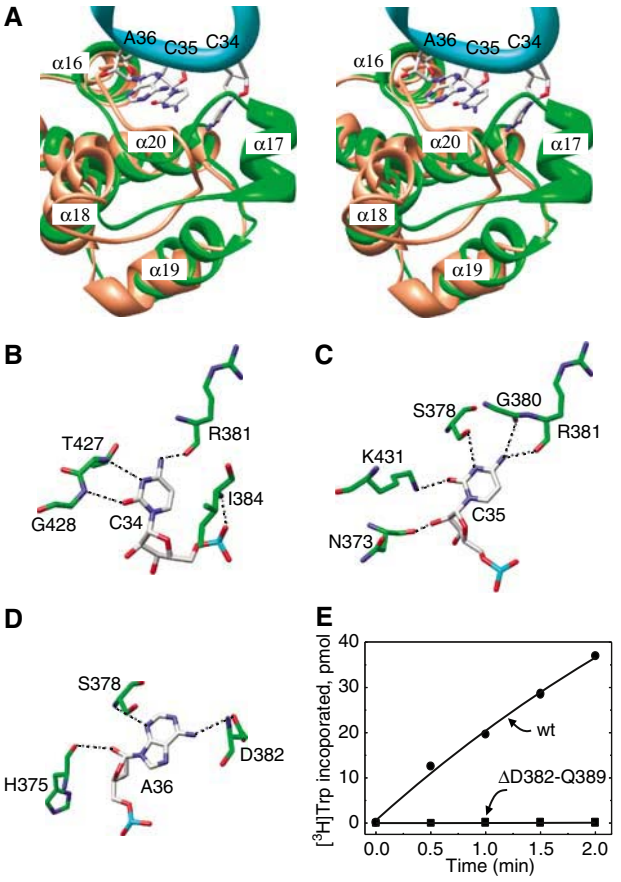

Figure 7 (**A**) Stereoview of TrpRS–tRNA^{Trp} interactions at the anticodon CCA. The *B. stearothermophilus* TrpRS structure (brown) is superimposed with the human TrpRS structure (green), showing the overall similarity except for the absence of helix α17 in the *B. stearothermophilus* TrpRS structure. (**B**–**D**) Recognitions of the three bases of the anticodon. (**E**) Deletion of helix α17 (ΔD382-Q389) on mini-TrpRS resulted in loss of aminoacylation activity.

(Figure 7D). Overall, only three out of nine base-protein hydrogen bonds employ protein side chains, whereas the other six use backbone interactions. Possibly, the heavy involvement of main chain atoms in the anticodon interaction makes recognition more resistant to mutation.

The conformation of the anticodon recognition domain of human TrpRS in the two complexes resembles that of *B. stearothermophilus* TrpRS (Doublie *et al*, 1995; Ilyin *et al*, 2000; Retailleau *et al*, 2001; Retailleau *et al*, 2003). However, helix α17 is absent in the latter structure (Kise *et al*, 2004) (Figure 7A). This helix in human TrpRS was suggested to be responsible for the antiangiogenic activity associated with mini-TrpRS (Kise *et al*, 2004), the N-terminal truncated splice variant with full aminoacylation activity. In our studies, deletion of α17 (ΔD382-Q389) from human mini-TrpRS resulted in loss of aminoacylation activity (Figure 7E) while the adenylate formation step was unaffected (data not shown). This observation is in contrast to that suggested by Kise *et al* (2004), but is not surprising because many residues on or near α17, that is, G380, R381, D382 and I384, are directly involved in anticodon interactions.

Even though the sequences of most anticodon recognition residues are not conserved between human and *B. stearothermophilus* TrpRS (Figure 4), superposition of *B. stearothermophilus* TrpRS (PDB 1I6L) (Retailleau *et al*, 2001) with the human complex structure revealed that all anticodon interactions, other than those that involve the α17 region, are likely to be conserved for bacterial TrpRS. This conservation is a consequence of most hydrogen-bonding interactions involving the backbone atoms. Interestingly, of the three residues with side chain interactions (S378, D382, K431), S378 and K431 are conserved among all three taxonomic domains. Position 378 has either S or T, both with a hydrogen donating OH group, and position 431 strictly has a K.

The anticodon interactions with R381, D382, and I384 of human TrpRS emanate from helix α17 and therefore are missing in *B. stearothermophilus* TrpRS. Interestingly, a long loop of 16 residues between helices α16 and α18 in *B. stearothermophilus* is similar in length to what is between α16 and α18 of human TrpRS, where helix α17 is embedded (Figure 7A). The α16–α18 loop of *B. stearothermophilus* TrpRS may undergo a tRNA-induced conformational change to fulfill the interactions with the anticodon.

Tryptophan binding pocket

Like the interactions with the anticodon, the tryptophan binding pocket containing the bound amino acid is the same in both complexes. The bound tryptophan is in an active site pocket in the middle of the Rossmann fold. Having partially been predicted (Yu *et al*, 2004), interactions with tryptophan have several interesting features, particularly when compared to the complex of tryptophan with *B. stearothermophilus* TrpRS (Retailleau *et al*, 2003). The indole nitrogen of the bound tryptophan forms a bifurcated hydrogen bond to the hydroxyl group of Y159 and to the side chain carbonyl group of Q194. The α-amino nitrogen forms two hydrogen bonds to the side chain carbonyl groups of E199 and Q284, respectively (Figure 5B). In contrast, different residues and fewer hydrogen bonds are involved in tryptophan recognition in *B. stearothermophilus* TrpRS (PDB 1MB2) (Retailleau *et al*, 2003). The indole nitrogen bonds to D132 and the α-amino nitrogen bonds to Y125. (D132 and Y125 correspond to P287 and F280 in human TrpRS.) With F5, C38, M129 and H43 replacing the four hydrogen-bonding residues in human TrpRS, the tryptophan-binding pocket appears to be more hydrophobic in *B. stearothermophilus* TrpRS (Figure 5C). Given that tryptophan binds with a similar affinity to eukaryotic and prokaryotic TrpRSs (Merle *et al*, 1984; Jia *et al*, 2002; Ewalt *et al*, 2005), hydrophobic interactions may play a more important role in *B. stearothermophilus* TrpRS than in human TrpRS, in order to compensate for weaker hydrogen bonding interactions in *B. stearothermophilus* TrpRS. The difference in mode of tryptophan binding by the two orthologs of TrpRS provides a structural rationale for designing antibiotics that specifically inhibit prokaryotic TrpRS. Indolmycin, a tryptophan analog containing an oxazolone ring joined to indole, is a natural example. It selectively inhibits prokaryotic TrpRS with an affinity at least 10^3-fold greater than that for eukaryotic TrpRS (Werner *et al*, 1976).

Association complex is closely similar to complex of uncharged tRNA^{Tyr} with TyrRS

As stated earlier, the initial crystallization sample of TrpRS with tRNA^{Trp} contained equal amounts of charged and uncharged tRNA^{Trp}, raising the possibility that the two bound

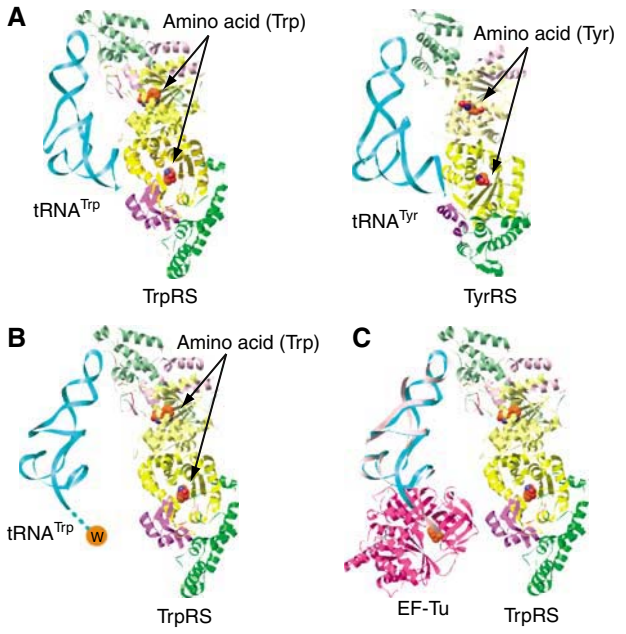

Figure 8 (**A**) The association TrpRS–tRNA^{Trp} complex (left) is closely similar to the uncharged tRNA complex of TyrRS (right, PDB 1J1U), suggesting that the association complex presented here contains uncharged tRNA^{Trp}. The second, symmetrically bound, tRNA is omitted for clarity. (**B**) The dissociation TrpRS–tRNA^{Trp} complex is shown with the presumptive amino acid attached to the tRNA. Only charged tRNA is forced off the active site upon new amino acid (Trp) binding, and this results in the dissociation conformation. (**C**) Model of the potential tertiary complex between human TrpRS, Trp-tRNA^{Trp} and EF-1α (ortholog of bacterial EF-Tu in eukaryotes). The dissociation complex is suitable for interacting with EF-1α, which selectively binds to only charged tRNAs. Phe-tRNA^{Phe} (pink) of the EF-Tu complex is superimposed with the dissociation tRNA^{Trp} (blue) of the TrpRS complex, with no steric hindrance found between EF-Tu and TrpRS. The model of the tertiary complex suggests that the elongation factor interacts with the patch of residues that are specific to eukaryotic TrpRSs.

tRNA conformations corresponded to charged and uncharged tRNA^{Trp}. Direct comparisons of the association complex with the uncharged tRNA^{Tyr} complex with TyrRS (Kobayashi *et al*, 2003) showed the two complexes to be virtually identical in the position of bound tRNA on the synthetase (Figure 8A). This comparison is especially helpful, because TyrRS and TrpRS are close homologs, being more similar (in sequence and structure) to each other than to any other class I tRNA synthetase (Doublie *et al*, 1995; Yang *et al*, 2003). As the complex of TyrRS with tRNA^{Tyr} was prepared from a solution lacking ATP, the bound tRNA^{Tyr} is *prima facie* uncharged. With these considerations in mind, we surmise that association complex presented here contains uncharged tRNA^{Trp}.

This conclusion is further strengthened by examining the more detailed orientation of the 3′-CCA end proposed for the TyrRS–(uncharged) tRNA^{Tyr} complex and seeing whether that orientation can be accommodated by the association complex. In the two previous TyrRS–tRNA^{Tyr} complexes (Yaremchuk *et al*, 2002; Kobayashi *et al*, 2003), the 3′-CCA end was disordered, reflecting a dynamic aminoacylation process. The same disorder of the 3′-CCA is seen here for the association complex, consistent with previous findings that C74 and C75 of the 3′-CCA were not protected by bovine TrpRS against alkylation (Garret *et al*, 1984). A model of the 3′-CCA for tRNA^{Tyr}, consistent with the biochemical data (Labouze and Bedouelle, 1989), was proposed to represent the conformation of the substrate in the active site right before the charging occurs (Labouze and Bedouelle, 1989; Yaremchuk *et al*, 2002). When the tRNA^{Tyr} molecule with the modeled 3′-CCA (S Cusack, personal communication) was superimposed onto tRNA^{Trp} of the association complex, the 2′-OH of the terminal ribose was placed adjacent to the carboxyl group of the bound tryptophan. Thus, even when examined at this level of detail, the associative tRNA^{Trp} exactly fits with being in the 'uncharged' conformation. (Notably, conformational rearrangement of the β1–β2 hairpin is likely to occur at the moment of charging, as its current conformation causes steric clashes with C75.)

Dissociation complex most likely caused by release of charged tRNA and is suitable for EF-1α binding

Tryptophan was shown to bind competitively with charged tRNA^{Trp} (Trp-tRNA^{Trp}) to bovine TrpRS (Trezeguet *et al*, 1986). As a consequence, Trp promoted dissociation of nascent Trp-tRNA^{Trp} from bovine TrpRS (Merle *et al*, 1988). (Similarly, in the related class I IleRS, at least three independent experiments showed that, after aminoacylation, the binding of a new molecule of isoleucine promoted the dissociation of Ile-tRNA^{Ile} (Yarus and Berg, 1969; Eldred and Schimmel, 1972; Eldred and Schimmel, 1973).) A density for tryptophan was found in the amino acid binding pocket of both the association and the dissociation complexes, suggesting that, most likely, the dissociative tRNA^{Trp} was charged at the time the crystal was being formed, and therefore was expelled from the active site by binding of a new tryptophan (Figure 8B). (When the crystal was dissolved, unsurprisingly, Trp attached to tRNA^{Trp} was not detected, presumably because it was lost by spontaneous deacylation, which happens rapidly at the pH of our crystallization (Schuber and Pinck, 1974) after the crystal was formed. Of course, unlike in solution, once the dissociation conformation is captured in the crystal, the crystal lattice interactions prevent the tRNA from recharging.) In contrast, because the associative tRNA^{Trp} was uncharged, it was not released from the active site when tryptophan was bound.

In the scheme of protein synthesis, after aminoacylation, EF-Tu in bacteria and its EF-1α ortholog in eukaryotes bind charged tRNAs and deliver them to the ribosome. In the complex cellular milieu of eukaryotes, it has long been thought that mechanisms for efficient transfer of products of one reaction to the enzyme, or factor, for the next are likely to have evolved. The reported interaction between TrpRS and EF-1α (Sang Lee *et al*, 2002) suggested a potential for such transfer, especially because TrpRS is one of the tRNA synthetases in mammals that appears not to occur in the multisynthetase complex (Kisselev, 1993). Enzymes in that complex may gain access to EF-1α by a different, shared mechanism.

As stated above, the orientation of the anticodon stem-loop of tRNA^{Trp} overlaps well between the two complexes (Figure 3). In the dissociation complex, the remainder of the tRNA outside of the anticodon loop is gradually separated from the synthetase. The acceptor stem is about 20 Å away from the protein, completely free of interactions (Figure 8B). Assuming the interaction between EF-Tu and Phe-tRNA^{Phe} in *Thermus thermophilus* (Nissen *et al*, 1995) is conserved for

eukaryotic elongation factor EF-1α (which has more than 30 % sequence identity to and a structure similar to bacterial EF-Tu (Andersen *et al*, 2000)), the dissociation complex can accommodate EF-1α binding to fit perfectly to the free (dissociated) acceptor stem (Figure 8C). Interestingly, this model suggests that EF-1α interacts with the patch of residues that are specific to eukaryotic TrpRSs (Figure 8C). The WHEP-TRS domain that is disordered here may also be involved in the interaction with the elongation factor.

Discussion

The capture of two sharply different dockings of bound tRNA in a single crystal demonstrates a remarkably versatile interaction surface of the two-domain L-shaped tRNA. (A subtle and localized dual tRNA conformation (with similar tRNA docking) in a LeuRS-$tRNA^{Leu}$ crystal was noted recently by Fukunaga and Yokoyama (2005).) That tRNA in this report can be loosely tethered to the synthetase through the anticodon alone is consistent with observations showing that anticodon-bearing stem-loop RNA oligonucleotides, in isolation, can bind to certain class I tRNA synthetases (Frugier *et al*, 1992; Gale and Schimmel, 1995). Further, the principle of microscopic reversibility requires that the tethering of tRNA to the enzyme through the anticodon in the dissociation complex is also the way that this tRNA makes initial contact with the synthetase, namely, through the anticodon-containing domain. Although not reported previously for either a class I or class II tRNA synthetase, this concept that initial tRNA binding is via the anticodon was proposed in light of several class II synthetase–tRNA complex structures from *T. thermophilus* (Cusack *et al*, 1996; Briand *et al*, 2000; Yaremchuk *et al*, 2000), where partial dissociation (and/or disordering) of the acceptor stem from the synthetase was observed. In those cases, however, the extent that the acceptor stems dissociated from the synthetase was more limited. Moreover, the partial dissociation of the acceptor stem was believed to be caused either by the lack of small substrates (like ATP or amino acid) that may be required to induce a productive enzyme conformation for acceptor stem binding or, instead, by the rigidity of the thermophilic enzyme when placed at low temperatures.

The idea suggested by the present structures is that the acceptor stem-containing domain is last to dock to the synthetase and is the first to dissociate. This concept is particularly significant for the interaction of charged tRNA with EF-1α. If the acceptor stem were first to dock and last to dissociate, then a direct 'hand-off' of the AA-tRNA to EF-1α would not be possible. The capability for hand-off from human TrpRS to the elongation factor is not likely to be unique to this synthetase, and probably requires at least a few specific contacts between the two proteins. Significantly, an interaction between EF-1α with each of several different mammalian tRNA synthetases has been directly demonstrated or inferred (Bec *et al*, 1989; Motorin *et al*, 1991; Reed *et al*, 1994; Negrutskii *et al*, 1996, 1999).

Materials and methods

Crystallization, data collection and structure determination

Human TrpRS was prepared as described (Wakasugi *et al*, 2002), and maintained in a stock solution of 10 mM HEPES (pH 7.5), 20 mM KCl, 0.02% NaN_3 and 2 mM β-mercaptoethanol. Bovine $tRNA^{Trp}$ transcript was prepared by *in vitro* transcription and purified by electrophoresis using a procedure detailed previously (Liu *et al*, 2002). The bovine $tRNA^{Trp}$ sequence shares all of its identity elements with human $tRNA^{Trp}$, and is a good substrate for aminoacylation by human TrpRS (Ewalt *et al*, 2005). The $tRNA^{Trp}$ was maintained in a stock solution of 20 mM Na cacodylate (pH 6.0) with 20 mM $MgCl_2$, and was annealed before use. The complex sample with 50% charged tRNA contained 230 μM of TrpRS, 250 μM of $tRNA^{Trp}$, 5 mM tryptophan and 10 mM AMP-PNP. Initial crystallization trials were conducted using the proprietary high throughput protein crystallization platform developed at Syrrx, Inc. (La Jolla, CA) as described before (Yang *et al*, 2002). Single crystals were obtained by vapor diffusion of sitting drops (2 μl of complex sample and 2 μl of reservoir solution) against a reservoir of 2 M ammonium sulfate and 0.1 M HEPES (pH 6.9) at 4°C. Selenium-labeled crystals were obtained in the same way using selenomethionine-containing protein prepared as described (Hendrickson *et al*, 1990).

The structure of the complex was determined by the SAD method using a selenium-labeled crystal. Synchrotron data were collected with beamline 5.0.2 at the Advanced Light Source of Lawrence Berkeley National Laboratory. Data were integrated and scaled with HKL2000 (Otwinowski and Minor, 1997). Twenty selenium sites were identified using SOLVE (Terwilliger and Berendzen, 1999). After density modification in RESOLVE (Terwilliger, 2000), the overall figure of merit at 2.9 Å increased from 0.43 to 0.59. Five hundred and sixty-eight protein residues were automatically built by RESOLVE, which covered about 73% of the protein residues in the final model. The remaining model of the complex including tRNAs and tryptophan substrates were built manually in O (Jones *et al*, 1991). The refinement was performed in CNS (Adams *et al*, 1998) with a final $R_{work} = 20.2\%$ and $R_{free} = 25.4\%$ at 2.9 Å. Data collection and refinement statistics of human TrpRS are summarized in Supplementary Table 1.

$tRNA^{Trp}$ analysis

Acid gel experiments were performed with various complex samples, including the sample of dissolved crystals, which were washed with mother liquor four times before being dissolved with 10 μl of a buffer containing 10 mM Na acetate (pH 4.5) and 1 mM EDTA. Charged and uncharged tRNAs were separated by acid urea polyacrylamide gel electrophoresis, by virtue of the difference in electrophoretic mobility between the two species (Varshney *et al*, 1991). The tRNAs are then electroblotted onto Hybond-N+ membrane (Amersham, Piscataway, NY) and detected by RNA blot hybridization. Membranes were prehybridized at 42°C for 6 h in a solution containing 10× Denhardt's, 6× SSC and 0.5% sodium dodecyl sulfate (SDS). Hybridization was performed at 42°C in 6× SSC and 0.1% SDS, and in the presence of a 5′-^{32}P-labeled oligonucleotide probe complementary to anticodon stem-loop sequence of $tRNA^{Trp}$. Membranes were washed at room temperature, once for 10 min in 6× SSC and 0.1% SDS, followed by one wash for 10 min in 6× SSC, and then subjected to autoradiography. Northern blots were quantified by PhosphorImager analysis using ImageQuant software (Amersham).

Preparation of α17 deletion mutant and the aminoacylation assay

Plasmid carrying a deletion mutant of mini-TrpRS (ΔD382–Q389) was generated with a QuikChange site-directed mutagenesis kit (Stratagene, La Jolla, CA). Protein concentration was evaluated by Bradford protein assay and active site titration. TrpRS variants were tested at the same active site concentrations. Aminoacylation reactions were carried out at 37°C and initiated by adding the enzyme to a final concentration of 10 nM to a reaction mixture containing 50 mM HEPES (pH 7.5) 20 mM KCl, 25 mM $MgCl_2$, 5 mM ATP, 5 μM [^{3}H]tryptophan, 20 mM β-mercaptoethanol, 0.2 mg/ml BSA and 2 μM bovine $tRNA^{Trp}$ transcript. Samples were collected at various times and spotted onto Whatman filters that had previously been soaked with 0.2% tryptophan in 5% trichloroacetic acid and dried. The filters were washed three times with 5% trichloroacetic acid and twice with ethanol before scintillation counting.

Data deposition

The atomic coordinates and structure factors have been deposited in the Protein Data Bank, www.rcsb.org (PDB ID code 2AZX).

Supplementary data
Supplementary data are available at *The EMBO Journal* Online.

Acknowledgements

We thank Dr Stephen Cusack for helpful discussions on this work, Dr Jamie M Bacher for comments on the manuscript, Drs Xiaoping Dai and Marc Elsliger for technical help. This work was supported by Grant GM 15539 from the National Institute of Health and a fellowship from the National Foundation for Cancer Research to P Schimmel and Grant R37-GM17151 from the National Institutes of Health to UL RajBhandary. ALS is supported by the US Department of Energy (DOE) under contract DE-AC03-76SF00098.

References

Adams PD, Rice LM, Brunger AT (1998) Crystallography & NMR system: a new software suite for macromolecular structure determination. *Curr Opin Struct Biol* **8:** 606–611

Andersen GR, Pedersen L, Valente L, Chatterjee I, Kinzy TG, Kjeldgaard M, Nyborg J (2000) Structural basis for nucleotide exchange and competition with tRNA in the yeast elongation factor complex eEF1A:eEF1Balpha. *Mol Cell* **6:** 1261–1266

Arnez JG, Moras D (1997) Structural and functional considerations of the aminoacylation reaction. *Trends Biochem Sci* **22:** 211–216

Bateman A, Birney E, Cerruti L, Durbin R, Etwiller L, Eddy SR, Griffiths-Jones S, Howe KL, Marshall M, Sonnhammer EL (2002) The Pfam protein families database. *Nucleic Acids Res* **30:** 276–280

Bec G, Kerjan P, Zha XD, Waller JP (1989) Valyl-tRNA synthetase from rabbit liver. I. Purification as a heterotypic complex in association with elongation factor 1. *J Biol Chem* **264:** 21131–21137

Bedouelle H, Guez-Ivanier V, Nageotte R (1993) Discrimination between transfer-RNAs by tyrosyl-tRNA synthetase. *Biochimie* **75:** 1099–1108

Briand C, Poterszman A, Eiler S, Webster G, Thierry J, Moras D (2000) An intermediate step in the recognition of tRNA(Asp) by aspartyl-tRNA synthetase. *J Mol Biol* **299:** 1051–1060

Carter Jr CW (1993) Cognition, mechanism, and evolutionary relationships in aminoacyl-tRNA synthetases. *Annu Rev Biochem* **62:** 715–748

Cusack S (1995) Eleven down and nine to go. *Nat Struct Biol* **2:** 824–831

Cusack S, Yaremchuk A, Tukalo M (1996) The crystal structures of *T. thermophilus* lysyl-tRNA synthetase complexed with *E. coli* tRNA(Lys) and a *T. thermophilus* tRNA(Lys) transcript: anticodon recognition and conformational changes upon binding of a lysyl-adenylate analogue. *EMBO J* **15:** 6321–6334

Doublie S, Bricogne G, Gilmore C, Carter Jr CW (1995) Tryptophanyl-tRNA synthetase crystal structure reveals an unexpected homology to tyrosyl-tRNA synthetase. *Structure* **3:** 17–31

Eldred EW, Schimmel PR (1972) Rapid deacylation by isoleucyl transfer ribonucleic acid synthetase of isoleucine-specific transfer ribonucleic acid aminoacylated with valine. *J Biol Chem* **247:** 2961–2964

Eldred EW, Schimmel PR (1973) Release of aminoacyl transfer ribonucleic acid from transfer ribonucleic acid synthetase studied by rapid molecular sieve chromatography. *Anal Biochem* **51:** 229–239

Ewalt KL, Yang XL, Otero FJ, Liu J, Slike B, Schimmel P (2005) Variant of human enzyme sequesters reactive intermediate. *Biochemistry* **44:** 4216–4221

Frugier M, Florentz C, Giegé R (1992) Anticodon-independent aminoacylation of an RNA minihelix with valine. *Proc Natl Acad Sci USA* **89:** 3990–3994

Fukunaga R, Yokoyama S (2005) Aminoacylation complex structure of leucyl-tRNA synthetase and $tRNA^{Leu}$ reveal two modes of discriminator-base recognition. *Nat Struct Mol Biol* **12:** 915–922

Gale AJ, Schimmel P (1995) Isolated RNA binding domain of a class I tRNA synthetase. *Biochemistry* **34:** 8896–8903

Garret M, Labouesse B, Litvak S, Romby P, Ebel JP, Giege R (1984) Tertiary structure of animal $tRNA^{Trp}$ in solution and interaction of $tRNA^{Trp}$ with tryptophanyl-tRNA synthetase. *Eur J Biochem* **138:** 67–75

Guo Q, Gong Q, Tong KL, Vestergaard B, Costa A, Desgres J, Wong M, Grosjean H, Zhu G, Wong JT, Xue H (2002) Recognition by tryptophanyl-tRNA synthetases of discriminator base on $tRNA^{Trp}$ from three biological domains. *J Biol Chem* **277:** 14343–14349

Hendrickson WA, Horton JR, LeMaster DM (1990) Selenomethionyl proteins produced for analysis by multiwavelength anomalous diffraction (MAD): a vehicle for direct determination of three-dimensional structure. *EMBO J* **9:** 1665–1672

Ilyin VA, Temple B, Hu M, Li G, Yin Y, Vachette P, Carter Jr CW (2000) 2.9 A crystal structure of ligand-free tryptophanyl-tRNA synthetase: domain movements fragment the adenine nucleotide binding site. *Protein Sci* **9:** 218–231

Jeong EJ, Hwang GS, Kim KH, Kim MJ, Kim S, Kim KS (2000) Structural analysis of multifunctional peptide motifs in human bifunctional tRNA synthetase: identification of RNA-binding residues and functional implications for tandem repeats. *Biochemistry* **39:** 15775–15782

Jia J, Chen XL, Guo LT, Yu YD, Ding JP, Jin YX (2004) Residues Lys-149 and Glu-153 switch the aminoacylation of tRNA(Trp) in *Bacillus subtilis*. *J Biol Chem* **279:** 41960–41965

Jia J, Xu F, Chen X, Chen L, Jin Y, Wang DT (2002) Two essential regions for tRNA recognition in *Bacillus subtilis* tryptophanyl-tRNA synthetase. *Biochem J* **365:** 749–756

Jones TA, Zou JY, Cowan SW, Kjeldgaard M (1991) Improved methods for building protein models in electron density maps and the location of errors in these models. *Acta Crystallogr A* **47:** 110–119

Kise Y, Lee SW, Park SG, Fukai S, Sengoku T, Ishii R, Yokoyama S, Kim S, Nureki O (2004) A short peptide insertion crucial for angiostatic activity of human tryptophanyl-tRNA synthetase. *Nat Struct Mol Biol* **11:** 149–156

Kisselev LL (1993) Mammalian tryptophanyl-tRNA synthetases. *Biochimie* **75:** 1027–1039

Kobayashi T, Nureki O, Ishitani R, Yaremchuk A, Tukalo M, Cusack S, Sakamoto K, Yokoyama S (2003) Structural basis for orthogonal tRNA specificities of tyrosyl-tRNA synthetases for genetic code expansion. *Nat Struct Biol* **10:** 425–432

Labouze E, Bedouelle H (1989) Structural and kinetic bases for the recognition of $tRNA^{Tyr}$ by tyrosyl-tRNA synthetase. *J Mol Biol* **205:** 729–735

Lee CP, RajBhandary UL (1991) Mutants of *Escherichia coli* initiator tRNA that suppress amber codons in *Saccharomyces cerevisiae* and are aminoacylated with tyrosine by yeast extracts. *Proc Natl Acad Sci USA* **88:** 11378–11382

Lee SW, Cho BH, Park SG, Kim S (2004) Aminoacyl-tRNA synthetase complexes: beyond translation. *J Cell Sci* **117:** 3725–3734

Liu J, Yang XL, Ewalt KL, Schimmel P (2002) Mutational switching of a yeast tRNA synthetase into a mammalian-like synthetase cytokine. *Biochemistry* **41:** 14232–14237

Merle M, Graves PV, Labouesse B (1984) Substrate depletion analysis as an approach to the pre-steady-state anticooperative kinetics of aminoacyl adenylate formation by tryptophanyl-tRNA synthetase from beef pancreas. *Biochemistry* **23:** 1716–1723

Merle M, Trezeguet V, Gandar JC, Labouesse B (1988) Effects of the ligands of beef tryptophanyl-tRNA synthetase on the elementary steps of the tRNA(Trp) aminoacylation. *Biochemistry* **27:** 2244–2252

Motorin YA, Wolfson AD, Lohr D, Orlovsky AF, Gladilin KL (1991) Purification and properties of a high-molecular-mass complex between Val-tRNA synthetase and the heavy form of elongation factor 1 from mammalian cells. *Eur J Biochem* **201:** 325–331

Myers CA, Kuhla B, Cusack S, Lambowitz AM (2002) tRNA-like recognition of group I introns by a tyrosyl-tRNA synthetase. *Proc Natl Acad Sci USA* **99:** 2630–2635

Negrutskii BS, Budkevich TV, Shalak VF, Turkovskaya GV, El'Skaya AV (1996) Rabbit translation elongation factor 1 alpha stimulates the activity of homologous aminoacyl-tRNA synthetase. *FEBS Lett* **382:** 18–20

Negrutskii BS, Shalak VF, Kerjan P, El'skaya AV, Mirande M (1999) Functional interaction of mammalian valyl-tRNA synthetase with elongation factor EF-1alpha in the complex with EF-1H. *J Biol Chem* **274:** 4545–4550

Nissen P, Kjeldgaard M, Thirup S, Polekhina G, Reshetnikova L, Clark BF, Nyborg J (1995) Crystal structure of the ternary complex of Phe-tRNAPhe, EF-Tu, and a GTP analog. *Science* **270:** 1464–1472

Otwinowski Z, Minor W (1997) Processing of X-ray diffraction data collected in oscillation mode. *Methods Enzymol* **276:** 307–326

Park SG, Ewalt KL, Kim S (2005) Functional expansion of aminoacyl-tRNA synthetases and their interacting factors: new perspectives on housekeepers. *Trends Biochem Sci* **30:** 569–574

Petrushenko ZM, Budkevich TV, Shalak VF, Negrutskii BS, El'skaya AV (2002) Novel complexes of mammalian translation elongation factor eEF1A. GDP with uncharged tRNA and aminoacyl-tRNA synthetase. Implications for tRNA channeling. *Eur J Biochem* **269:** 4811–4818

Reed VS, Wastney ME, Yang DC (1994) Mechanisms of the transfer of aminoacyl-tRNA from aminoacyl-tRNA synthetase to the elongation factor 1 alpha. *J Biol Chem* **269:** 32932–32936

Retailleau P, Huang X, Yin Y, Hu M, Weinreb V, Vachette P, Vonrhein C, Bricogne G, Roversi P, Ilyin V, Carter Jr CW (2003) Interconversion of ATP binding and conformational free energies by tryptophanyl-tRNA synthetase: structures of ATP bound to open and closed, pre-transition-state conformations. *J Mol Biol* **325:** 39–63

Retailleau P, Yin Y, Hu M, Roach J, Bricogne G, Vonrhein C, Roversi P, Blanc E, Sweet RM, Carter Jr CW (2001) High-resolution experimental phases for tryptophanyl-tRNA synthetase (TrpRS) complexed with tryptophanyl-3′AMP. *Acta Crystallogr D* **57:** 1595–1608

Ribas de Pouplana L, Schimmel P (2001) Aminoacyl-tRNA synthetases: potential markers of genetic code development. *Trends Biochem Sci* **26:** 591–596

Sampath P, Mazumder B, Seshadri V, Gerber CA, Chavatte L, Kinter M, Ting SM, Dignam JD, Kim S, Driscoll DM, Fox PL (2004) Noncanonical function of glutamyl-prolyl-tRNA synthetase: gene-specific silencing of translation. *Cell* **119:** 195–208

Sang Lee J, Gyu Park S, Park H, Seol W, Lee S, Kim S (2002) Interaction network of human aminoacyl-tRNA synthetases and subunits of elongation factor 1 complex. *Biochem Biophys Res Commun* **291:** 158–164

Sankaranarayanan R, Moras D (2001) The fidelity of the translation of the genetic code. *Acta Biochim Pol* **48:** 323–335

Schimmel P, Ribas de Pouplana L (2001) Formation of two classes of tRNA synthetases in relation to editing functions and genetic code. *Cold Spring Harbor Symp Quant Biol* **66:** 161–166

Schuber F, Pinck M (1974) On the chemical reactivity of aminoacyl-tRNA ester bond. I. Influence of pH and nature of the acyl group on the rate of hydrolysis. *Biochimie* **56:** 383–390

Terwilliger TC (2000) Maximum-likelihood density modification. *Acta Crystallogr D* **56:** 965–972

Terwilliger TC, Berendzen J (1999) Automated MAD and MIR structure solution. *Acta Crystallogr D* **55:** 849–861

Torres-Larios A, Dock-Bregeon AC, Romby P, Rees B, Sankaranarayanan R, Caillet J, Springer M, Ehresmann C, Ehresmann B, Moras D (2002) Structural basis of translational control by *Escherichia coli* threonyl tRNA synthetase. *Nat Struct Biol* **9:** 343–347

Trezeguet V, Merle M, Gandar JC, Labouesse B (1986) Kinetic evidence for half-of-the-sites reactivity in $tRNA^{Trp}$ aminoacylation by tryptophanyl-tRNA synthetase from beef pancreas. *Biochemistry* **25:** 7125–7136

Varshney U, Lee CP, RajBhandary UL (1991) Direct analysis of aminoacylation levels of tRNAs *in vivo*. Application to studying recognition of *Escherichia coli* initiator tRNA mutants by glutaminyl-tRNA synthetase. *J Biol Chem* **266:** 24712–24718

Wakasugi K, Slike BM, Hood J, Otani A, Ewalt KL, Friedlander M, Cheresh DA, Schimmel P (2002) A human aminoacyl-tRNA synthetase as a regulator of angiogenesis. *Proc Natl Acad Sci USA* **99:** 173–177

Werner RG, Thorpe LF, Reuter W, Nierhaus KH (1976) Indolmycin inhibits prokaryotic tryptophanyl-tRNA ligase. *Eur J Biochem* **68:** 1–3

Xu F, Chen X, Xin L, Chen L, Jin Y, Wang D (2001) Species-specific differences in the operational RNA code for aminoacylation of tRNA(Trp). *Nucleic Acids Res* **29:** 4125–4133

Xue H, Shen W, Giege R, Wong JT (1993) Identity elements of tRNA(Trp). Identification and evolutionary conservation. *J Biol Chem* **268:** 9316–9322

Yang XL, Otero FJ, Skene RJ, McRee DE, Schimmel P, Ribas de Pouplana L (2003) Crystal structures that suggest late development of genetic code components for differentiating aromatic side chains. *Proc Natl Acad Sci USA* **100:** 15376–15380

Yang XL, Schimmel P, Ewalt KL (2004) Relationship of two human tRNA synthetases used in cell signaling. *Trends Biochem Sci* **29:** 250–256

Yang XL, Skene RJ, McRee DE, Schimmel P (2002) Crystal structure of a human aminoacyl-tRNA synthetase cytokine. *Proc Natl Acad Sci USA* **99:** 15369–15374

Yaremchuk A, Cusack S, Tukalo M (2000) Crystal structure of a eukaryote/archaeon-like protyl-tRNA synthetase and its complex with tRNAPro(CGG). *EMBO J* **19:** 4745–4758

Yaremchuk A, Kriklivyi I, Tukalo M, Cusack S (2002) Class I tyrosyl-tRNA synthetase has a class II mode of cognate tRNA recognition. *EMBO J* **21:** 3829–3840

Yarus M, Berg P (1969) Recognition of tRNA by isoleucyl-tRNA synthetase. Effect of substrates on the dynamics of tRNA-enzyme interaction. *J Mol Biol* **42:** 171–189

Yu Y, Liu Y, Shen N, Xu X, Xu F, Jia J, Jin Y, Arnold E, Ding J (2004) Crystal structure of human tryptophanyl-tRNA synthetase catalytic fragment: insights into substrate recognition, tRNA binding, and angiogenesis activity. *J Biol Chem* **279:** 8378–8388